Mass-Transfer Effects in the Biphasic Hydroformylation of Propylene

Cents, A.H.G.; Brilman, D.W.F.; Versteeg, G.F.

Published in:
Industrial & Engineering Chemistry Research

DOI:
10.1021/ie049888g

Publication date:
2004

Mass-Transfer Effects in the Biphasic Hydroformylation of Propylene

A. H. G. Cents, D. W. F. Brilman, and G. F. Versteeg*

OOIP Group, Department of Chemical Engineering, University of Twente, P.O. Box 217, 7500 AE Enschede, The Netherlands

The hydroformylation of propylene to butyraldehyde is an important industrial process. In this reaction system, carbon monoxide, hydrogen, and propylene are converted to *n*-butyraldehyde in an aqueous phase containing a water-soluble rhodium catalyst. This reaction system consists therefore of three different phases: the aqueous catalyst phase, the organic butyraldehyde phase, and the gas phase. A modeling study indicated that an optimum value of the production rate is reached at a certain power input. It was shown that mass transfer plays an important role in this reaction system and that accurate knowledge of the mass-transfer parameters in the gas−liquid−liquid system is necessary to predict and to optimize the production rate. Mass-transfer experiments with CO, H_2, and propylene in water and in solutions consisting of water with different amounts of *n*-butyraldehyde were carried out in a stirred autoclave. The results indicated that the addition of small amounts of butyraldehyde caused a relatively small increase increase in k_La, which was probably caused by a larger increase of the gas−liquid interfacial area, a, accompanied by a decrease in the mass-transfer coefficient, k_L. Near the point of maximum solubility of butyraldehyde, a strong (factor of 3) increase in k_La was observed. The most logical explanation for this is an increase in k_L, because measurement of the interfacial area did not show such an increase. This increase in k_L, i.e., the disappearance of the initial decrease, might be due to the disappearance of the rigid layer of butyraldehyde molecules at the gas−liquid interface by formation and spreading of a butyraldehyde layer around the bubble.

1. Introduction

The biphasic hydroformylation of propylene was first reported by Kuntz.[1] Its major advantage over the conventional single-phase hydroformylation process is the higher selectivity (95% compared to 80%) to the desired product, *n*-butyraldehyde. The reaction scheme is shown in Figure 1. The reaction is carried out in the aqueous phase containing a rhodium catalyst with water-soluble ligands. The product butyraldehyde is sparingly soluble and forms a second (dispersed) liquid phase. This catalyst is made water-soluble by the addition of triphenylphosphine-*m*-trisulfonic acid trisodium salt (TPPTS).

The biphasic hydroformylation of propylene has been commercially applied by Ruhrchemie/Rhône-Poulenc (RC/RP, currently Hoechst/Celanese) since 1984. A schematic outline of the process is presented in Figure 2, and the estimated relevant process parameters[2,3] are listed in Table 1. In this process, syngas and propylene are fed to a reactor in which the conversion to butyraldehyde takes place. In the reactor, a system of three phases exists: the aqueous phase containing the catalyst; a dispersed phase containing butyraldehyde; and a gas phase consisting of the gaseous reactants CO, H_2, and propylene. After leaving the reactor, the reaction mixture is transported to a gas−liquid separator in which the unconverted gases are separated from the liquids and returned to the reactor. The liquid two-phase system is separated by simple decantation, and the aqueous catalyst phase is transported back to the reactor. Impurities are removed from the organic phase

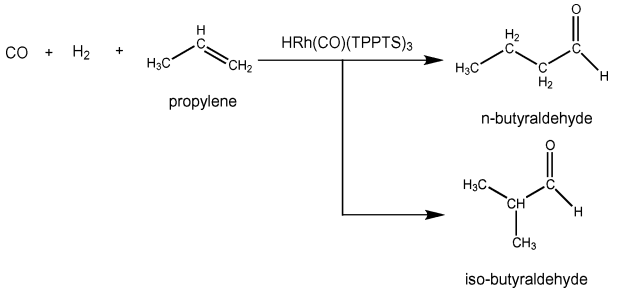

Figure 1. Scheme of the reaction in the biphasic hydroformylation of propylene using a rhodium catalyst.

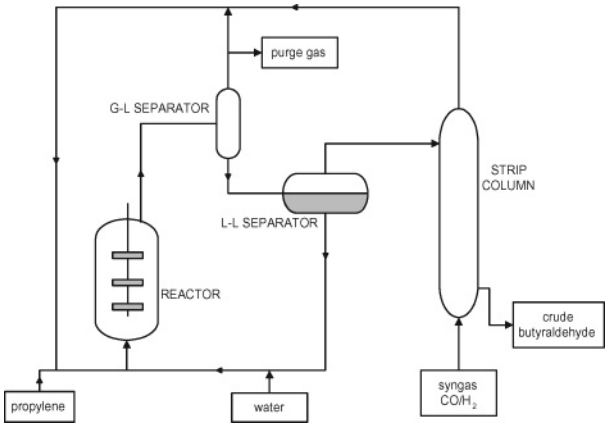

Figure 2. Simplified process scheme of the RC/RP biphasic hydroformylation of propylene.

in a stripping column using the syngas stream. The crude butyraldehyde can be further processed to a distillation column in which the *n*-butyraldehyde is

* To whom correspondence should be addressed. E-mail: g.f.versteeg@utwente.nl.

10.1021/ie049888g CCC: $27.50
Published on Web 10/15/2004

Table 1. Estimated Relevant Process Parameters of the RC/RP Biphasic Hydroformylation of Propylene

parameter	value
temperature, °C	120
pressure, bar	10−50
rhodium concentration, ppm	300−1000
normal/iso ratio	(13−30):1

separated from the iso form. Strengths of this process are the low rhodium losses (less than 10^{-9} g/kg of *n*-butyraldehyde[4]) and the low energy consumption.

Butyraldehyde is a versatile product, and the raw material can be used for the production of numerous other chemicals. A major part of the produced butyraldehyde is converted to butanols and 2-ethylhexanol, and butyraldehyde is also used as the raw material for the production of carboxylic acids and amines.

The influence of mass transfer in this process was investigated by Wachsen et al.[5] These authors concluded from their experimental work that the process was (at least partially) mass-transfer-limited. With the development of improved, more active catalysts[6] mass transfer will be increasingly important in this reaction system.

In this article, the influence of the volume fraction of butyraldehyde on the volumetric mass-transfer coefficient in the biphasic hydroformylation of propylene is investigated. In the first part of this article (sections 2 and 3), a modeling study in which mass transfer and reaction kinetics were taken into account is described. In the second part of this article (sections 4−6), mass-transfer experiments involving the different gases found in the hydroformylation reaction (CO, H_2, and propylene) into water with different fractions butyraldehyde are described.

2. Modeling of Mass Transfer and Chemical Reaction

The model that is used in this section takes both the mass transfer and the chemical reaction into account. The governing equations that determine the fluxes of the three gases (A = H_2, B = CO, and E = propylene) into the aqueous liquid phase are as follows

$$\frac{dc_A}{dt} = D_A \frac{d^2c_A}{dx^2} - R_A \tag{1}$$

$$\frac{dc_B}{dt} = D_B \frac{d^2c_B}{dx^2} - R_B \tag{2}$$

$$\frac{dc_E}{dt} = D_E \frac{d^2c_E}{dx^2} - R_E \tag{3}$$

with boundary conditions

$t = 0, x > 0$:
$c_A(x,t) = c_{A,bulk}, \quad c_B(x,t) = c_{B,bulk}, \quad c_E(x,t) = c_{E,bulk}$

$t > 0, x = 0$:
$c_A(x,t) = m_A c_{A,G}, \quad c_B(x,t) = m_B c_{B,G}, \quad c_E(x,t) = m_E c_{E,G}$

$t > 0, x = \infty$:
$c_A(x,t) = c_{A,bulk}, \quad c_B(x,t) = c_{B,bulk}, \quad c_E(x,t) = c_{E,bulk}$

Table 2. Kinetic Parameters as Determined by Yang et al.[7]

parameter	value	parameter	value
k_0[a]	7.545×10^{12}	k_2	0.5641
E_A	83.15	k_3[b]	0.4995
k_1	1.367	k_4	1.823×10^{-2}

[a] The units of R_X, E_A, c, and the partial pressures (p_i) in eq 7 are mol/(m^3 s), kJ/mol, mol/m^3, and bar, respectively. [b] The partial pressure of propylene, p_E, is at 16 °C. Other pressures are at reaction temperature.

From these equations, the fluxes of the different gases into the liquid can be calculated according to

$$J(t) = D \left.\frac{dc(t)}{dx}\right|_{x=0} \tag{4}$$

The average flux in time can be determined using the penetration model

$$\bar{J} = \frac{1}{\tau_p}\int_0^{\tau_p} J(t)\, dt \tag{5}$$

In the reactor model, a constant partial pressure of the gaseous reactants was assumed, and the overall losses of CO, H_2, and propylene from the liquid phase were neglected. In the steady state, the fluxes of all components are then equal to the total reaction rate in the solution

$$R_X = \bar{J}_A a = \bar{J}_B a = \bar{J}_E a \tag{6}$$

The bulk concentrations of the three different reactants can be determined from this equation.

2.1. Kinetics. The kinetics of the hydroformylation reaction in the presence of a $RhCl(CO)(TPPTS)_2$/TPPTS complex catalyst were experimentally determined by Yang et al.[7] These authors varied the propylene concentration, the initial pressure, the H_2/CO ratio, the temperature, the rhodium concentration, and the ligand/rhodium ratio in an orthogonal experimental design to obtain the following rate expression

$$R_X = k_0 \exp\left(\frac{-E_A}{RT}\right) \times \frac{p_A p_B p_E c_{Rh}}{(1 + k_1 p_A)(1 + k_2 p_B)^2 (1 + k_3 p_E)^2 (1 + k_4 c_{Lig})^3} \tag{7}$$

The constants are defined in Table 2. The concentrations of the three different gases were calculated from the partial pressures using the Peng−Robinson equation of state with standard mixing rules to combine the kinetic rate expression with the flux calculations.

2.2. Mass Transfer. A standard stirred-tank contactor with Rushton-type agitator and baffles is used in the present study to determine the mass-transfer properties for the absorption of the three hydroformylation gases in the water−butyraldehyde solution. This vessel was characterized completely in terms of gas hold-up, bubble size, interfacial area, and mass-transfer coefficient for coalescing as well as noncoalescing systems. The addition of butyraldehyde to water is likely to prevent coalescence of gas bubbles in the solution (because of the strong decrease in surface tension, from 72.8 to 37.6 mN/m at 25 °C[8]), which means that the results obtained and correlations recommended for the

noncoalescing system are most appropriate. The bubble diameter can probably be best described with the equation proposed by Calderbank[9] for aliphatic alcohol solutions

$$d_{32} = 1.90\left[\frac{\sigma^{0.6}}{\left(\frac{P_g}{V}\right)^{0.4}\rho^{0.2}}\right]\epsilon^{0.65}\left(\frac{\mu_G}{\mu_L}\right)^{0.25} \quad (8)$$

The gassed power input can be calculated from the relation given by Hughmark[10]

$$\frac{P_g}{P} = 0.10\left(\frac{\Phi_G}{NV}\right)^{-1/4}\left(\frac{N^2 D_I{}^4}{WgV^{2/3}}\right)^{-1/5} \quad (9)$$

The gas hold-up in noncoalescing systems has been given by Greaves and Barigou[11]

$$\epsilon = 3.86N^{0.92}\Phi_G{}^{0.41}\left(\frac{D_I}{T_V}\right)^{2.56} \quad (10)$$

The interfacial area is calculated using the relation $a = 6\epsilon/d_{32}$. The mass-transfer coefficient, k_L, is calculated according to the work of Linek et al.,[12] using a correction for the diffusion coefficient

$$k_{L,W} = 2 \times 10^{-4}\left(\frac{P_g}{V}\right)^{0.14}\left(\frac{D^T}{D_{O_2}{}^{25}}\right)^{0.67} \quad (11)$$

It is well-known that the addition of surfactant-like components (such as butyraldehyde) reduces surface tension, and such components can form a somewhat stagnant, more rigid layer of molecules around the bubble. This hydrodynamic effect causes a decrease in the mass-transfer coefficient. Llorens et al.[13] investigated this behavior and found the following relation

$$\text{for } 0.4 < \pi < 16 \text{ mN/m} \qquad \frac{k_L}{k_{L,W}} = \frac{1}{1.25 + 73\pi} \quad (12)$$

$$\text{for } \pi > 16 \text{ mN/m} \qquad \frac{k_L}{k_{L,W}} = 0.41 \quad (13)$$

in which π (N/m) is the interfacial pressure, defined as $\pi = \sigma_W - \sigma$.

This k_L value can be used in the calculation of the penetration time according to

$$\tau_p = \frac{4D}{\pi k_L{}^2} \quad (14)$$

2.3. Dispersed Phase. The addition of a dispersed phase can increase the rate of mass transfer when the solubility of the component to be transferred is higher in the dispersed phase than in the continuous phase. Cents et al.[14] have shown that this increase of mass transfer in the case of toluene and 1-octanol could be well described using a homogeneous model of the shuttle mechanism. When it is assumed that this description is also applicable to the biphasic hydroformylation of propylene with butyraldehyde as the dispersed phase, the governing equations are

$$[1 + \epsilon_D(m_{R,A} - 1)]\frac{dc_A}{dt} = D_A\frac{d^2c_A}{dx^2} - (1 - \epsilon_D)R_X \quad (15)$$

$$[1 + \epsilon_D(m_{R,B} - 1)]\frac{dc_B}{dt} = D_B\frac{d^2c_B}{dx^2} - (1 - \epsilon_D)R_X \quad (16)$$

$$[1 + \epsilon_D(m_{R,E} - 1)]\frac{dc_E}{dt} = D_E\frac{d^2c_E}{dx^2} - (1 - \epsilon_D)R_X \quad (17)$$

The boundary conditions are similar compared to those for the system without a dispersed phase. The following assumptions are made: (1) The dispersed phase is equally divided throughout the gas−liquid mass-transfer zone. (2) The concentration of each of the three gases in the dispersed phase is, at any time and place within the mass-transfer zone, at equilibrium with its concentration in the surrounding continuous phase. (3) The presence of the microphase droplets does not influence the surface renewal frequency of the continuous liquid phase.

Neglecting the liquid−liquid mass transfer is likely to be justified, because of the low water−butyraldehyde interfacial tension. This means that the butyraldehyde droplets are very small, thus creating a high liquid−liquid interfacial area. Assumption 3 seems reasonable as Cents et al.[14] found that, for all dispersed liquid phases, whether or not they enhanced mass transfer, the apparent k_L value remained constant.

2.4. Numerical. The bulk concentrations of the different gases can be determined starting with an empty bulk and increasing the bulk concentration using the average flux after each penetration time until a steady-state situation is reached. In this situation (with and without a dispersed phase), the following relation holds

$$(1 - \epsilon_D)R_X = \bar{J}_A a = \bar{J}_B a = \bar{J}_E a \quad (18)$$

Performing such a determination is, however, quite time-consuming, and in this case, an algorithm is used that calculates an initial guess of the bulk concentrations using the film model by solving the equation

$$R_X = k_L a(mc_G - c_{bulk})$$

or in the case in which a dispersed phase is present

$$R_X = k_L a\sqrt{1 + \epsilon_D(m_R - 1)}(mc_G - c_{bulk})$$

for all three components. Thereafter, the bulk concentrations are solved from eq 18 using the full set of equations in an optimization routine.

The set of three partial differential equations is solved using the method of lines. The system is converted to ordinary differential equations (ODEs) by central discretization of the diffusion term and solved using a variable-order, stiff ODE solver. The number of place steps (in the mass-transfer zone) was 50, and the number of times steps (during the penetration time) was 500. This combination gave good agreement with the analytical solution in a simple first-order reaction system, and increasing the number of steps did not influence the results. The penetration depth for physical absorption ($\delta_p = 4D/k_L$) was taken as 1.5 times the penetration depth of the gas with the largest diffusion

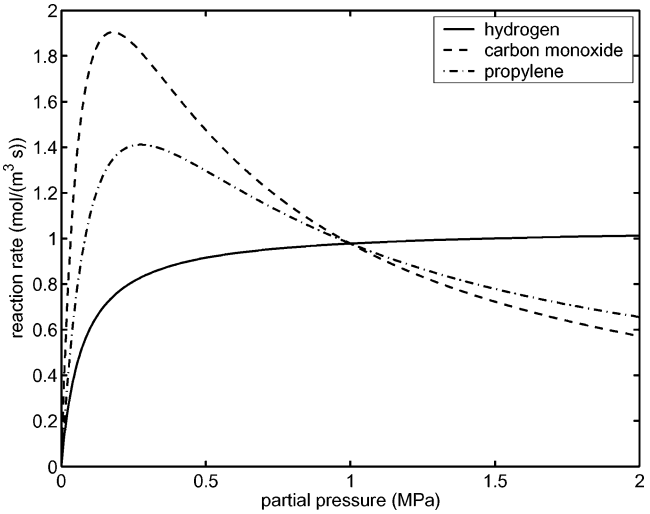

Figure 3. Effect of the partial pressures of H_2, CO, and propylene on the reaction rate.

coefficient (hydrogen), which verified that $dc/dx = 0$ at $x = \infty$. The flux was approximated as

$$J(t) = D(3c_0 - 4c_1 + c_2)/\Delta x^2$$

and the fluxes were integrated in time using the Simpson rule.

3. Modeling Results

3.1. Effect of Partial Pressure on Reaction Rate. The effect of the partial pressures of the three hydroformylation gases on the reaction rate (no mass-transfer limitations) is shown in Figure 3. The reaction rates are calculated for a temperature of 120 °C and partial pressures of 10 bar of H_2, 10 bar of CO, and 10 bar of propylene (at reaction temperature), unless the partial pressure is the parameter under investigation. Plots of the reaction rate versus partial pressure for CO and propylene show a maximum around 2−3 bar. At higher partial pressures, a decreasing rate is found with increasing partial pressure.

3.2. Effect of Catalyst Concentration. The effect of negative-order dependencies on the production rates can be significant when both mass transfer and chemical reaction are partially limiting. An example of such an effect is shown in Figure 4. In this figure, the reaction rate versus the gassed power input is plotted for three catalyst concentrations. The physical properties and operating conditions that were used are listed in Table 3. At low power input per unit volume, the rate increases with increasing power input; it then passes through a maximum and eventually becomes independent of the power input provided by the impeller. This kind of behavior was also observed by Bhattacharya and Chaudhari,[15] who studied the homogeneous one-phase hydroformylation of 1-hexene.

At low gassed power input, the mass transfer of CO is limiting (in this example), which means that the bulk concentration of CO remains almost zero. An example of the concentration profiles in the liquid phase at low power input at the end of the penetration time is provided in Figure 5. The mass-transfer rate is not enhanced by the reaction as no influence of the increased catalyst concentration is found at low values of the power input. The maximum in Figure 4 occurs at the conditions in which the bulk concentrations of CO

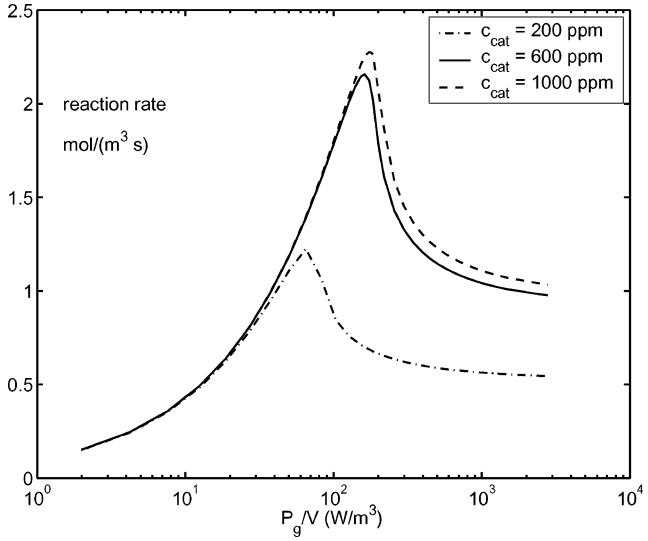

Figure 4. Reaction rate versus gassed power input at different rhodium concentrations.

Table 3. Physical Parameters and Operating Conditions Used in the Modeling Study of the Biphasic Hydroformylation of Propylene

parameter	value	units	parameter	value	units
T	120	°C	c_{Rh}	600	ppm
p_A	1.0[a]	MPa	c_{Lig}/c_{Rh}	30:1	
p_B	1.0[a]	MPa	m_A	0.022[b]	
p_E	1.0[a]	MPa	m_B	0.025[b]	
ρ_L	940	kg/m^3	m_E	0.050[b]	
μ_L	2.4	10^4 Pa s	$m_{R,A}$	6.4[b]	
μ_G	1.7	10^5 Pa s	$m_{R,B}$	9.6[b]	
σ[b]	0.027	N/m	$m_{R,E}$	48[b]	
D_A^{393}[d]	2.59	10^8 m^2/s	V	50	10^3 m^3
D_B^{393}[d]	1.60	10^8 m^2/s	u_G	0.58	10^2 m/s
D_E^{393}[d]	9.51	10^9 m^2/s			

[a] At reaction temperature, unless specified otherwise. [b] Estimated from the IUPAC solubility data series.[22] [c] Surface tension of water saturated with butyraldehyde. [d] Estimated using the Díaz equation.[23]

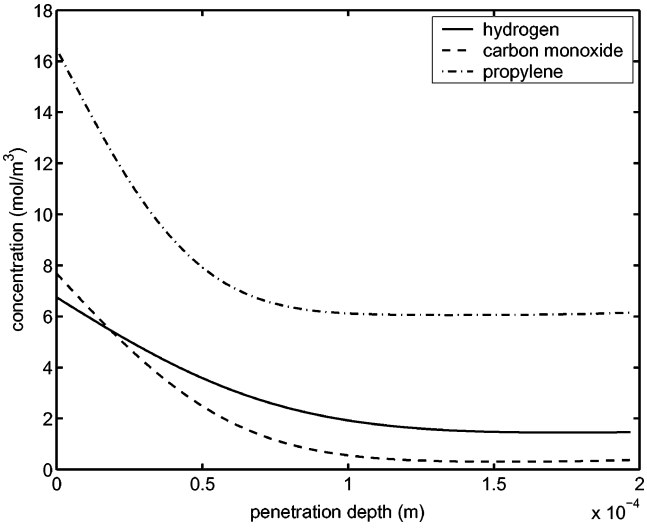

Figure 5. Concentration profiles in the liquid phase at $P_g = 50$ W/m^3 and operating conditions given in Table 3.

and propylene are at an optimum level (close to 2−3 bar or 20−30% of the saturation concentration). This maximum will occur at lower power inputs for lower catalyst concentrations, as the bulk concentrations will increase at lower power inputs at a lower rate. At high

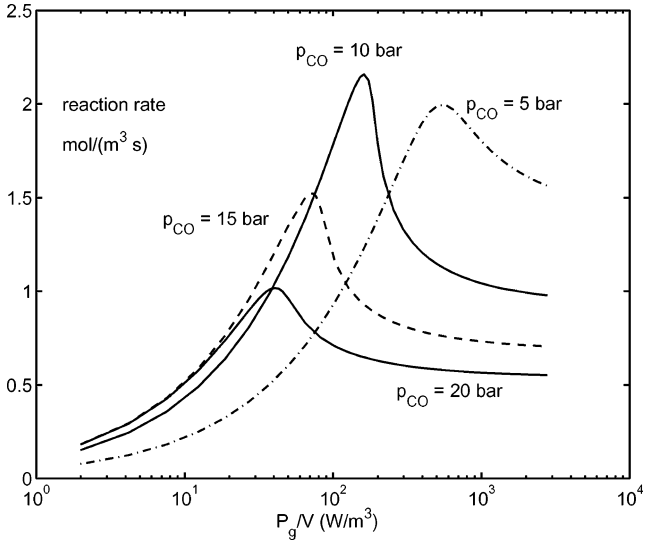

Figure 6. Reaction rate versus gassed power input at different CO partial pressures.

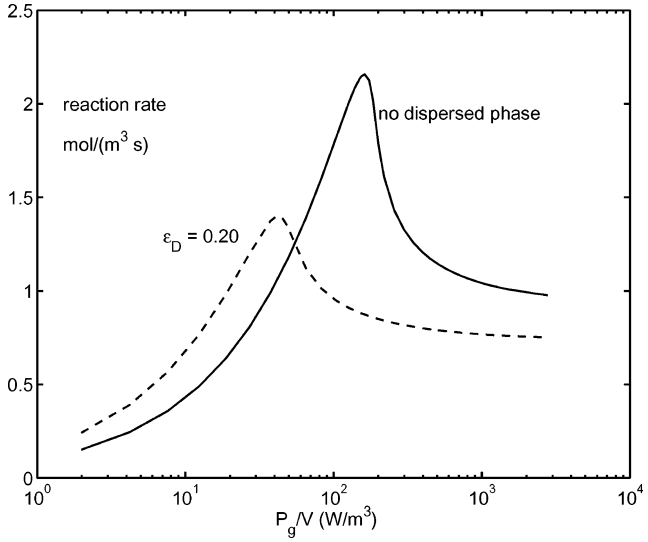

Figure 7. Influence of dispersed butyraldehyde on the reaction rate assuming a homogeneous model of the shuttle mechanism.

power inputs, the reaction rate is kinetically controlled, and all concentrations in the bulk are almost equal to the concentrations at the interface. A large increase in reaction rate is observed for an increase in rhodium content from 200 to 600 ppm. The increase in production rate occurring from 600 to 1000 ppm is much lower, mainly because of a larger reaction rate inhibition due to the higher ligand concentration.

3.3. Effect of CO Partial Pressure. The influence of the CO partial pressure on the reaction rate is shown in Figure 6. At low CO partial pressures (5 bar) and at low power inputs, the production rate suffers from severe CO mass-transfer limitations. The bulk concentration of CO is close to zero. The maximum production rate (at optimum CO and propylene bulk concentrations) is reached at a relatively high power input. This maximum production rate is lower than that observed in the case with 10 bar of CO, because of a less-optimal combination of CO and propylene bulk concentrations. At higher CO partial pressures (15 and 20 bar) and low power inputs, the reaction is limited not by CO mass transfer, but (in this example) by hydrogen mass transfer. The optimum production rate is reached at lower power inputs, at which the mass-transfer rate is still relatively low. A lower optimum production rate is therefore obtained. In this example, the optimum CO partial pressure seems to be around 10 bar. Further optimization of the production rate is possible.

3.4. Effect of the Dispersed Phase. The above modeling results show that, in this reaction system, the production rate is quite sensitive to the power input of the impeller. This means that accurate knowledge of the mass-transfer parameters is required to predict the correct concentration profiles and to optimize the production rate. It is known that the presence of a dispersed phase can change the concentration profiles and thereby the flux of the gaseous components to the aqueous phase (for instance, by the shuttle model). In Figure 7, the effect of 20 vol % dispersed butyraldehyde on the production rate is shown, assuming a homogeneous model of the shuttle mechanism. At low power inputs, the mass transfer is enhanced by the dispersed butyraldehyde, which has a higher solubility for the gases than the aqueous phase. This higher solubility decreases the concentration of the dissolved gases in the mass-transfer zone near the interphase, which leads to a higher gas-to-liquid flux. Because of the increased mass-transfer rate, compared to the case in which no dispersed phase is present, the concentrations *in the bulk* increase to this optimum level at lower power inputs, and the maximum productivity is reached when the flux is still rather low because of the low mass-transfer rate. The optimum production rate is lower in this case. When lower partial pressures are applied, the optimum will be at higher power inputs, and a higher production rate can be achieved. At high power inputs, the concentrations in the bulk are almost equal to the concentrations at the interphase for both cases. The production rate is lower when the dispersed phase is present, because of the lower continuous-phase volume available for the reaction to occur.

In a previous study,[14] it was shown that two components increased mass transfer (toluene and 1-octanol) and two organic liquids did not (*n*-heptane and *n*-dodecane). In the next section, experimental results of mass-transfer (absorption) experiments are presented for the three hydroformylation gases in water, water with dissolved butyraldehyde, and water−butyraldehyde dispersions. In this way, the influence of butyraldehyde on the mass-transfer coefficient $k_L a$ is investigated.

4. Experimental Section

Mass-transfer experiments were carried out in a 640-mL-capacity autoclave (Büchi) equipped with a gas-inducing turbine with a variable speed up to 2200 rpm. The gas was induced in the stirrer shaft by four holes in the top of the shaft and retrieved in the solution by four holes between two round plates on which the impeller blades were mounted. The total impeller diameter was 4.5 cm, and the blade width was 1 cm. The reactor was jacketed and temperature controlled by an oil bath up to 150 °C with an accuracy of 0.1 °C. A fast pressure transducer (up to 60 bar, 0.01 bar accuracy) was used to measure the pressure in the reactor. The temperatures and pressures were recorded on a PC. A schematic diagram of the setup is shown in Figure 8.

In a typical absorption experiment, the gas was introduced into a jacketed and stirred storage vessel;

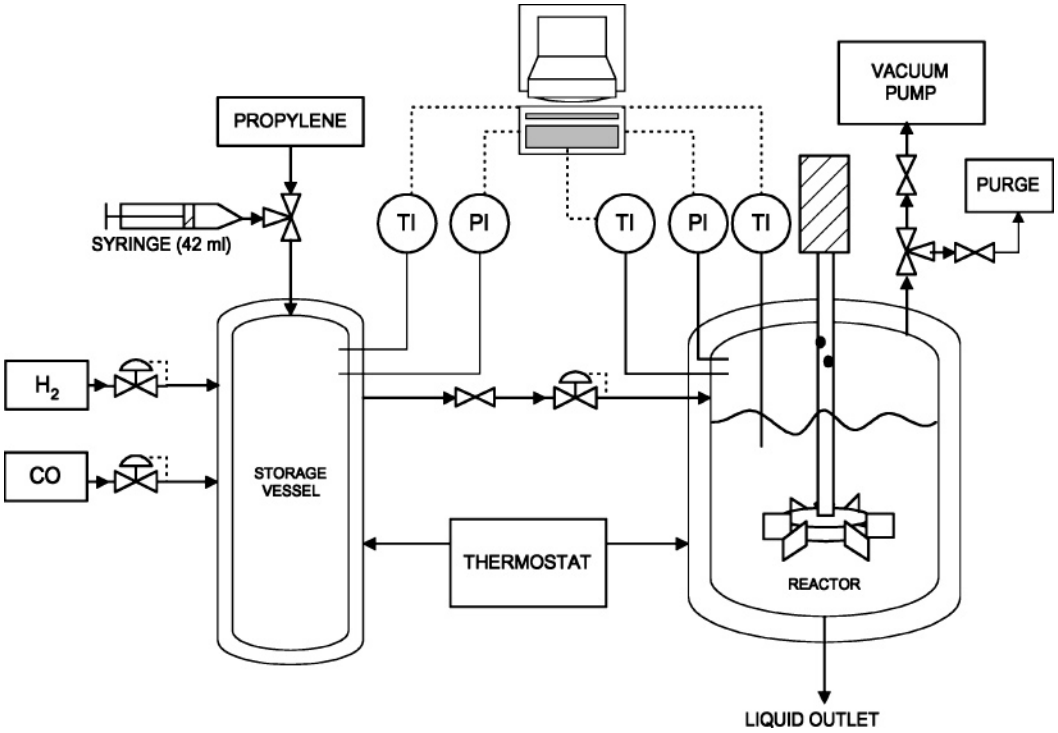

Figure 8. Schematic diagram of the setup.

hydrogen and carbon monoxide were taken from gas bottles by making use of a pressure reducer, and propylene was introduced as a liquid using a pressurized syringe. In the experiments with propylene, the storage vessel was heated to 120 °C at which point all of the propylene was in the gas phase. The experiments were performed below the vapor pressure of propylene at the measurement temperature to avoid condensation in the reactor. The gases were transported to the reactor using a pressure reducer at the desired pressure. The liquid in the vessel was degassed before the experiments by the application of vacuum. After the gas had been introduced into the reactor and the pressure had stabilized, the stirrer was switched on, and the pressure versus time curve was recorded on a personal computer. When a dispersed phase was present in the reactor, stirring was applied before the introduction of the gas to obtain a well-dispersed system at the start of the experiment. All experiments were performed at a temperature between 22 and 25 °C, a pressure of 8 bar (in the case of propylene, around 3 bar), and a stirring speed of 800 rpm.

4.1. Chemicals. The experiments were performed with *n*-butyraldehyde as the dispersed phase, because this is the main product in the biphasic hydroformylation of propylene. *N*-butyraldehyde was obtained from Merck with a purity higher than 99%. Deionized water was used as the continuous phase. All gases were obtained from Hoek Loos. Carbon monoxide had a purity of 99.997%, hydrogen had a purity of 99.999% and propylene had a purity of 99.8%.

4.2. Interpretation of the Mass-Transfer Experiments. In a gas−liquid system, the volumetric liquid-phase mass-transfer coefficient, k_La, is determined from the pressure drop by making use of a mole balance of the absorbed gas

$$\frac{dn_G}{dt} = -k_La\left[m\frac{n_G(t)}{V_G} - c_L(t)\right]V_L \qquad (19)$$

with boundary conditions

$$t = 0: \qquad n_G = n_{G,0}$$

$$t = \infty: \qquad n_G = n_{G,eq}$$

The measured pressures are converted to moles by using the Peng−Robinson equation of state. The concentration in the liquid phase can be determined from the number of moles that have been absorbed from the gas phase, according to the expression

$$c_L(t) = [n_{G,0} - n_G(t)]/V_L$$

Equation 19 can be integrated to obtain

$$k_Lat = -\frac{n_{G,eq}}{n_{G,0}}\ln\left[\frac{n_G(t) - n_{G,eq}}{n_{G,0} - n_{G,eq}}\right] = Y \qquad (20)$$

When the right-hand side of eq 20 is plotted versus time, the slope equals k_La. The distribution coefficient, m, can be determined according to

$$m = \frac{c_{L,eq}}{c_{G,eq}} = \frac{n_{G,0} - n_{G,eq}}{n_{G,eq}}\frac{V_G}{V_L} \qquad (21)$$

The determination of k_La is not as straightforward in gas−liquid−liquid (G−L−L) three-phase systems as in G−L two-phase systems. The driving force for mass transfer depends on the presence of butyraldehyde in the mass-transfer zone. The difference between these two situations is clarified in Figure 9. When the dispersed phase is present in the mass-transfer zone, the driving force is larger, and a smaller k_La value will be calculated from the experiments.

As in a one-phase system, the determination of the k_La (without dispersed phase in the mass-transfer zone, D1) starts with the mole balance of the absorbed gas (eq 19). The concentration in the continuous liquid phase

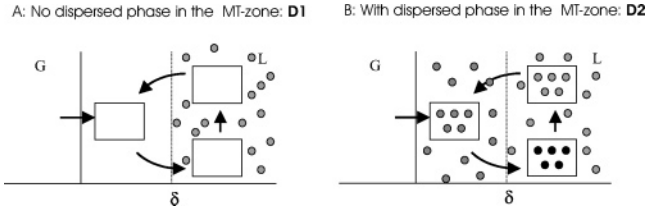

Figure 9. Mass transfer in systems with butyraldehyde as the dispersed phase.

is now given by

$$c_{L,C}(t) = \frac{n_{L,C}(t)}{V_L} = \frac{n_{G,0} - n_G(t) - n_{L,D}(t)}{V_L} \quad (22)$$

The number of moles in the dispersed phase can be determined using the definition of relative solubility

$$m_R = \frac{c_{L,D}(t)}{c_{L,C}(t)} = \frac{(1-\epsilon_D)}{\epsilon_D}\frac{n_{L,D}(t)}{n_{L,C}(t)} \quad (23)$$

By combining these two equations, the continuous liquid-phase concentration can be described by

$$c_{L,C}(t) = \frac{n_{G,0} - n_G(t)}{[1 + \epsilon_D(m_R - 1)]} \quad (24)$$

The volumetric mass-transfer coefficient in case of a dispersed phase, which is not present in the mass-transfer zone, can now be determined as

$$k_L a_{D1} t = -\frac{n_{G,eq}}{n_{G,0}} \ln\left[\frac{n_G(t) - n_{G,eq}}{n_{G,0} - n_{G,eq}}\right][1 + \epsilon_D(m_R - 1)] = Y_{D1} \quad (25)$$

The solubility in the continuous phase (saturated with butyraldehyde), m_C^*, can be calculated according to

$$m_C^* = \frac{c_{L,C,eq}}{c_{L,G,eq}} = \frac{1}{[1 + \epsilon_D(m_R - 1)]}\frac{V_G}{V_L}\frac{n_{G,0} - n_{G,eq}}{n_{G,eq}} \quad (26)$$

The solubility ratio, m_R, can be determined from measurements in the presence of a dispersed phase. In this case, the following relations hold

$$m_{ov} = (1 - \epsilon_D)m_C^* + \epsilon_D m_D^* \quad \text{and} \quad m_R = \frac{m_D^*}{m_C^*} \quad (27)$$

in which m_{ov} is the overall solubility ratio measured as if there was no dispersed phase present.

In the case in which dispersed-phase droplets are present in the mass-transfer zone (D2) and the mass transfer is enhanced according to a homogeneous model of the shuttle mechanism, $k_L a$ can be determined by making use of the enhancement factor proposed by Bruining et al.[16] The mass-transfer coefficient can be determined from the case without droplets in the mass-transfer zone (D1) and is given by

$$k_L a_{D2} = \frac{k_L a_{D1}}{\sqrt{1 + \epsilon_D(m_R - 1)}} \quad (28)$$

5. Results

In Figure 10, the results of two typical mass-transfer experiments are presented. One experiment is shown with 1.1 vol % butyraldehyde, which is less than the solubility of butyraldehyde in water (10.4 vol % at 25 °C[17]). The other experiment was performed with 25.6 vol % butyraldehyde and thus consisted of approximately 15% dispersed phase. The decrease in pressure was quite rapid in both cases. In most cases, a measurement time of 15 s was possible. After this, the changes in pressure were too small, and the Y versus time plot contained a great deal of scatter. From Figure 10, it can be seen that the value of $k_L a$ is about 3 times larger in the presence of the dispersed phase Than in the one-phase system. This phenomenon will be studied more intensively in the next sections.

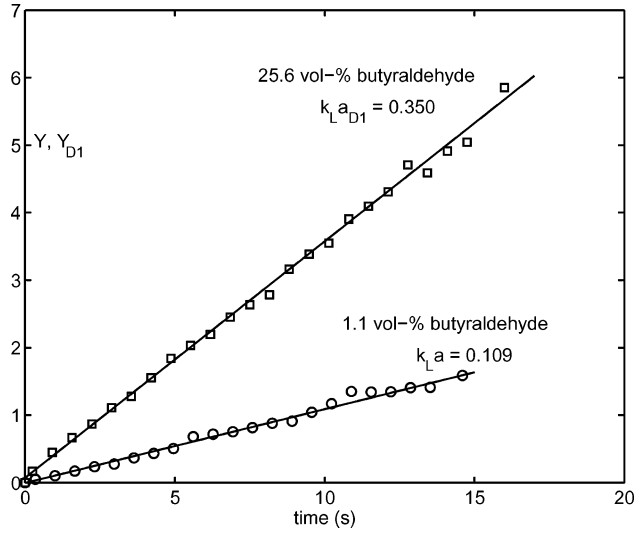

Figure 10. Linearity of the Y versus time plot in the measurement of $k_L a$ using the batchwise absorption method.

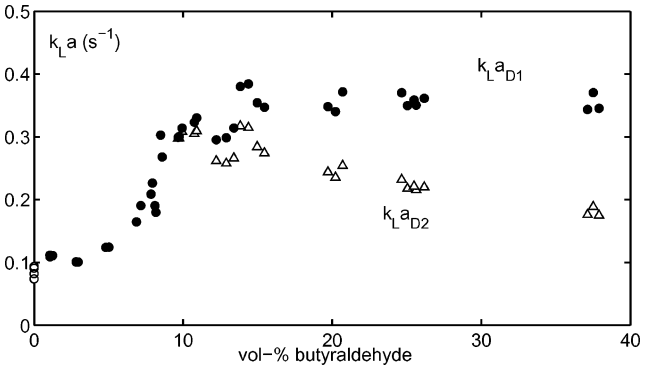

Figure 11. Effect of the butyraldehyde volume fraction on $k_L a$ of CO in ○, water; ●, water−butyraldehyde ($k_L a$, $k_L a_{D1}$); △, water−butyraldehyde ($k_L a_{D2}$).

5.1. Mass Transfer of Carbon Monoxide. The results for the relationship between $k_L a$ and the volume fraction of *n*-butyraldehyde in the case of carbon monoxide absorption are shown in Figure 11. Upon addition of a small amount of butyraldehyde, a small increase of $k_L a$ is observed. At low (1−6 vol %) butyraldehyde fractions, $k_L a$ remains relatively constant. At butyraldehyde fractions close to the maximum solubility of butyraldehyde in water (7−10 vol %), a sharp increase (approximately a factor of 3) in $k_L a$ is observed. At butyraldehyde fractions beyond the maximum solubility, no further enhancement of mass transfer is observed. The value of $k_L a_{D1}$ remained practically constant. Enhancement of mass transfer according to a homogeneous model of the shuttle mechanism is therefore

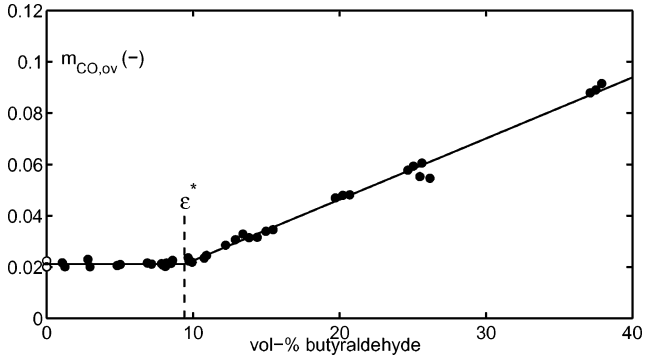

Figure 12. Effect of the butyraldehyde volume fraction on the solubility of CO in ○, water; ●, water−butyraldehyde.

Table 4. Solubilities and Mass-Transfer Coefficients of CO, H_2, and Propylene in Water and Butyraldehyde at 22−25 °C

parameter	CO	H_2	propylene
solubility in water, m_C	0.0208	0.0185	0.143
solubility in the aqueous phase, m_C^*	0.0211	0.0194	0.20
relative solubility, $m_R = m_D/m_C^*$	11.2	4.5	65.3
max. solubility of butyraldehyde, ϵ^* (%)	9.4	11.1	7.7
k_La in water, k_La (s^{-1})	0.085	0.075	0.052
k_La in the aqueous phase, k_La^* (s^{-1})	0.112	0.136	0.098
k_La after the maximum solubility, k_La_{D1} (s^{-1})	0.355	0.38	0.27

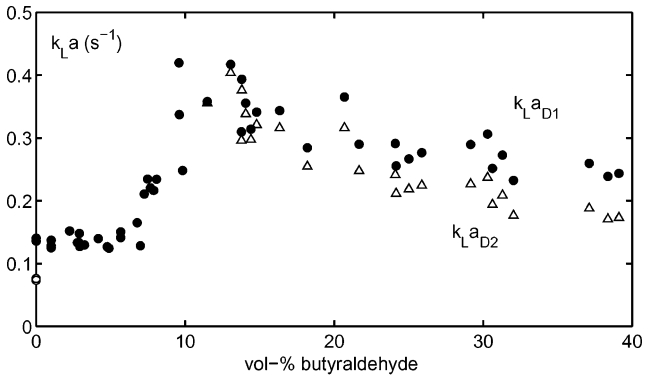

Figure 13. Effect of the butyraldehyde volume fraction on k_La of H_2 in ○, water; ●, water−butyraldehyde (k_La, k_La_{D1}); △, water−butyraldehyde (k_La_{D2}).

unlikely, and k_La_{D2} showed a decreasing trend with increasing butyraldehyde volume fraction.

From the plot of the overall solubility, m_{ov}, as shown in Figure 12, the solubilities of CO in the aqueous phase and in butyraldehyde can be determined. The solubility of CO in water is not affected by dissolved butyraldehyde. The maximum solubility of butyraldehyde in water can be determined as 9.5 vol %, which is somewhat smaller than the literature value of 10.4 vol %. Beyond the point of maximum solubility of butyraldehyde, $m_{ov,CO}$ increases linearly with dispersed-phase fraction. The physical properties that can be derived from these plots for all gases are reported in Table 4.

5.2. Mass Transfer of Hydrogen. The effect of the butyraldehyde volume fraction on the mass-transfer coefficient is shown in Figure 13. The addition of small fractions of butyraldehyde causes an increase in k_La of 80%, which is significantly greater than the increase observed in the experiments with carbon monoxide (30%). Similarly to the results with CO as the gas phase, a sharp increase in the mass-transfer coefficient was observed near the maximum solubility point. No enhancement of mass transfer was obtained after this point; rather, a decrease occurred. The value of the mass-transfer coefficient when a homogeneous model of the shuttle mechanism is applied (k_La_{D2}) is also shown in Figure 13, although the validity of this model in the case of a decreasing mass-transfer rate is not very realistic. The solubility of H_2 was approximately constant below the maximum butyraldehyde solubility (Table 4). Beyond this point, a linear increase in the overall solubility was obtained, similar to Figure 12. The value for the relative solubility, m_R, was 4.5, which was much lower than the value with CO (11.2).

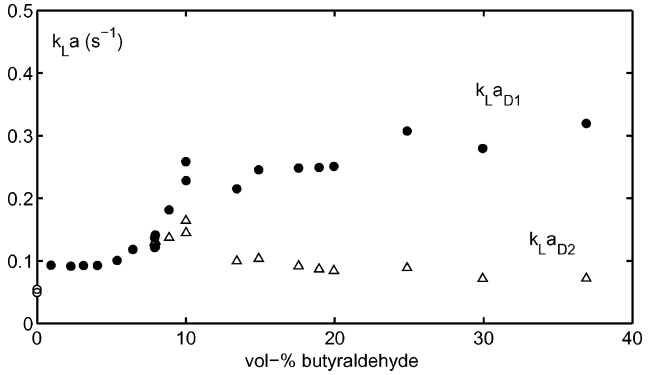

Figure 14. Effect of the butyraldehyde volume fraction on k_La of propylene in ○, water; ●, water−butyraldehyde (k_La, k_La_{D1}); △, water−butyraldehyde (k_La_{D2}).

5.3. Mass Transfer of Propylene. Mass-transfer experiments with propylene at 8 bar were more difficult than experiments with carbon monoxide and hydrogen. Both the solubility and the k_La value were dependent on the propylene concentration in the solution. This caused nonlinear plots of Y versus time and nonreproducible results. Therefore, the experiments were performed at a pressure of around 3 bar. At such pressures, the values of m and k_La were relatively independent of the gas-phase propylene pressure.

The mass-transfer coefficient, k_La, is plotted versus the volume fraction of butyraldehyde in Figure 14. A trend similar to that observed in the experiments with CO and H_2 was obtained. The value for k_La in the presence of dissolved butyraldehyde was approximately 90% higher than that in pure water. The point of maximum butyraldehyde solubility was reached at 7.7% according to the overall solubility plot. This value is somewhat lower than those for hydrogen and carbon monoxide, which might be due to the dissolved propylene in the solution. After the maximum solubility point, again, an increase by approximately a factor 3 is observed. At higher dispersed-phase fractions, the mass-transfer rate is somewhat higher (k_La_{D1}), but it is not likely that this enhancement is due to the shuttle mechanism, because a strongly decreasing trend in k_La_{D2} is observed. An enhancement due to the shuttle mechanism would result in a higher enhancement because of the high relative solubility in case of propylene.

6. Discussion

In the experiments with all three gases, a more or less similar trend was obtained for the volumetric liquid-phase mass-transfer coefficient, k_La, and for the volumetric liquid-phase mass-transfer coefficient in the presence of a dispersed phase, k_La_{D1}, which is shown in Figure 15. The increase in mass-transfer rate from pure water to water with dissolved butyraldehyde (A) varied from 30 to 90% depending on the gas. This increase in

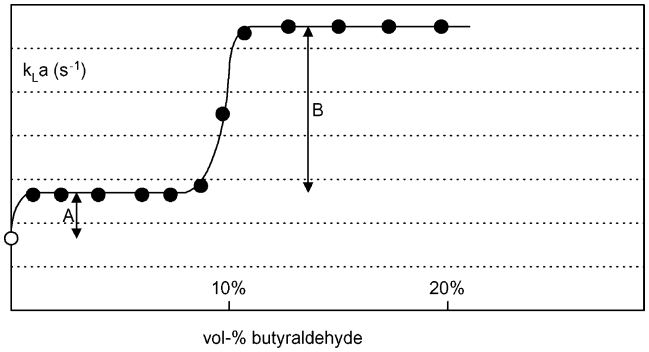

Figure 15. General trend in the mass-transfer experiments.

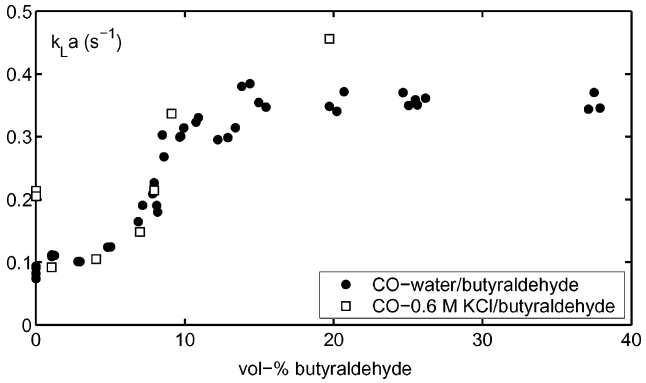

Figure 16. Effect of the butyraldehyde volume fraction on k_La and k_La_{D1} of CO in water−butyraldehyde and in 0.6 M KCl−butyraldehyde.

k_La is small compared to the expected increase in the interfacial area, a, according to mass-transfer correlations for coalescing and noncoalescing systems. It seems that the expected increase in interfacial area is accompanied by a decrease in the mass-transfer coefficient, k_L, as indicated in eq 13 from the work of Llorens et al.[13] To test this hypothesis, two types of additional experiments were carried out: (1) measurement of k_La in a noncoalescing electrolyte system and (2) measurement of the interfacial area using ultrasonic spectroscopy.

In the experiments with the noncoalescent electrolyte solution, 0.6 M KCl was used as the aqueous phase. This concentration was high enough to suppress coalescence according to the results of Craig et al.[18] The results with different fractions of butyraldehyde are given in Figure 16 and show that the value of k_La without butyraldehyde in the solution is much higher than the value in water. The addition of butyraldehyde caused a strong decrease in the volumetric mass-transfer coefficient to the level of the water−butyraldehyde system. This is most likely caused by a decrease in the mass-transfer coefficient, k_L, and not by a decrease in the interfacial area, a. The decrease in the mass-transfer coefficient is a factor 2.3, which is very close to the factor 2.4 that was predicted according to eq 13. With the exception of the experiments without butyraldehyde, the trend is approximately similar compared to that for the CO−water−butyraldehyde system.

It was, unfortunately, not possible to measure the gas−liquid interfacial in the autoclave that was used in these experiments. To obtain a qualitative impression of the interfacial area in water−butyraldehyde systems, measurements were performed in a 2-L glass reactor. Nitrogen was used as the dispersed gas phase. Measurements of the interfacial area were made using

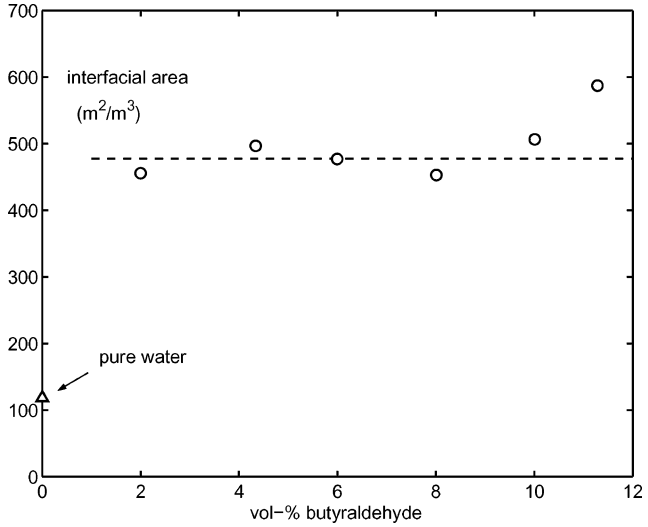

Figure 17. Effect of the butyraldehyde volume fraction on the gas−liquid interfacial area measured using ultrasonic spectroscopy.

ultrasonic spectroscopy. Details of this method can be found elsewhere.[19] These measurements indicated that the area in water containing butyraldehyde is approximately a factor 4 higher compared to the area in pure water. The results are shown in Figure 17. These results indicate that, together with the above-discussed decrease in k_L by a factor of 2.3, it seems that the small increase in k_La (A in Figure 15) upon addition of butyraldehyde to water is determined by two largely compensating effects: a decrease in k_L together with a increase in the interfacial area a. Beyond the point of maximum solubility, a small increase in a is observed, but this increase is not large enough to explain the sharp increase in k_La (B in Figure 15) that was obtained in the mass-transfer experiments.

The most logical explanation for the sharp increase in k_La at the point of maximum butyraldehyde solubility (B in Figure 15) is an increase in the mass-transfer coefficient, k_L. The increase is approximately a factor 2.5−3 for all gases. A further increase of the interfacial area is unlikely, as this increase was also not observed in the interfacial area measurements.

A possible explanation for the increase in the mass-transfer coefficient (step B in Figure 15) is that the rigid layer of molecules that is responsible for the original decrease in the mass-transfer coefficient has disappeared. This might be due to the formation of a larger butyraldehyde layer around the bubble. This layer is probably more mobile and therefore not able to suppress the turbulence acting on the bubble wall. The final spreading coefficient ($S^* = \sigma^*_{W/G} - \sigma^*_{O/G} - \sigma^*_{O/W}$), which indicates whether it is favorable for an organic layer to spread over a bubble under mutually saturated conditions, was determined using a Krüss K9 tensiometer and was positive (+7 mN/m). This indicates that the spreading of a butyraldehyde layer on a gas bubble is energetically favorable. Furthermore, it was shown that the presence of a small layer of butyraldehyde on the saturated solution decreased the spreading coefficient to approximately zero. Bartell et al.[20] showed that the formation of such a small layer can occur spontaneously, when the initial spreading coefficient is positive.

Beyond the point of maximum solubility, mass transfer was not enhanced by the addition of more butyraldehyde. This was found by Cents et al.[14] for the addition

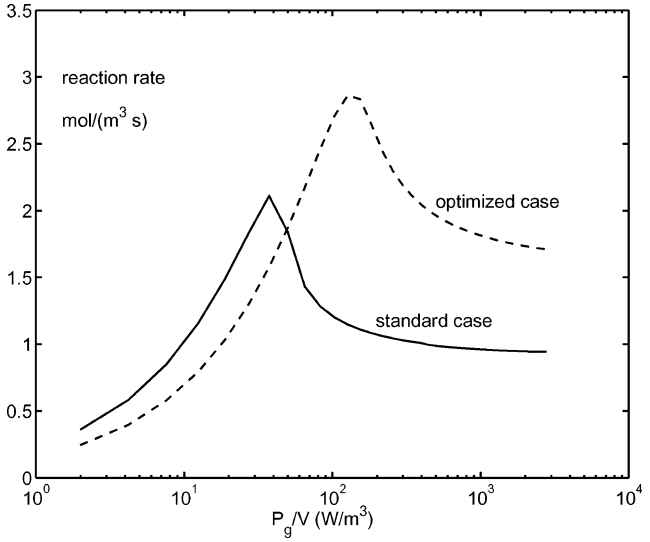

Figure 18. Optimized solution compared to the standard case. Optimum is at 140 W/m^3 with p_{H_2} = 36.9 bar, p_{CO} = 6.8 bar, $p_{propylene}$ = 6.3 bar, c_{Rh} = 0.92 mol/m^3, and c_{Rh}/c_{Lig} = 1:30.

of *n*-heptane and *n*-dodecane to an aqueous phase, whereas toluene and 1-octanol did enhance mass transfer, which could be well described using a homogeneous model of the shuttle mechanism. Furthermore, Lekhal et al.[21] found that mass transfer of hydrogen and carbon monoxide was enhanced according to the shuttle mechanism (the mass-transfer coefficient did not decrease while the effect of the dispersed phase was taken into account in their model) with octene as the dispersed phase. In their study, additional enhancement was observed around at a dispersed phase content of 3−4 vol %. These differences, which are not clearly understood, indicate that additional research on this topic is required, to be able to predict the influence of the dispersed phase on the rate of mass transfer.

For the modeling case, these results imply that the decrease in the mass-transfer coefficient should not be taken into account, as the reactor operates above the solubility limit (around 10 vol %). Furthermore, mass transfer is not enhanced at higher dispersed-phase fractions. These results can be used in the selection of the optimum process parameters for the biphasic hydroformylation of propylene (and probably for other biphasic hydroformylation reactions as well). Figure 18 shows that high production rate can be obtained at a relatively low power input compared to the standard case. For both cases, the reduction of k_L due to the butyraldehyde molecules was not taken into account. In optimizing the production rate, the following constraints were used: p_{tot} < 50 bar, T = 120 °C, c_{Rh} < 1.5 mol/m^3, and c_{Rh}/c_{Lig} > 1:30. An optimal production rate was achieved at a gassed power input of 140 W/m^3 and was almost 3 mol/(m^3 s).

7. Conclusions

In this work, a modeling study was performed on the biphasic hydroformylation of propylene to butyraldehyde. Because of the negative-order dependencies on the CO and propylene partial pressures in the kinetic rate expression, an unusual effect of the power input on the production rate was observed. The production rate first increased with increasing power input to an optimum value. Beyond this maximum, a decrease was observed to a value at which the concentrations in the liquid bulk were equal to the concentrations at the interface.

Furthermore, it was shown that the addition of a dispersed phase (in this case, butyraldehyde) can change the concentration profiles in the mass-transfer zone, which can cause a shift in the optimum production rate to lower power inputs. These examples show that accurate knowledge of the mass-transfer properties in gas−liquid−liquid systems is necessary to predict and optimize the production rate in the biphasic hydroformylation of propylene.

Experiments made clear that the addition of small amounts of butyraldehyde caused a relatively small increase in the volumetric mass-transfer coefficient, k_La. This small increase was due to a larger increase in the interfacial area, a, accompanied by a decrease in the mass-transfer coefficient, k_L. Near the point of the maximum solubility of butyraldehyde, a strong (factor of 3) increase in k_La was observed. The most logical explanation for this is an increase in k_L, as independent measurement of the interfacial area using an ultrasonic technique did not show such an increase in the surface area. This increase in k_L might be due to the disappearance of the rigid layer of butyraldehyde molecules at the gas−liquid interface by the spreading of a butyraldehyde layer around the bubble. This hypothesis was supported by surface tension measurements.

The results obtained in this work lead to an increased insight into the biphasic hydroformylation of propylene and can therefore be used to increase the production rate of this process.

Acknowledgment

The authors thank B. J. Frowijn and S. M. Biewenga for their assistance in the experimental work. B. Knaken is acknowledged for the construction of the experimental setup and for the technical support.

List of Symbols

a = gas−liquid interfacial area (m^2/m^3)
c_A = concentration of component A (mol/m^3)
D = diffusion coefficient of component A (m^2/s)
d_{32} = Sauter mean diameter (m)
D_I = diameter of the impeller (m)
E_A = activation energy (kJ/mol)
g = gravitational constant (9.81 m/s^2)
J_A = flux of component A [mol/(m^3 s)]
k_L = liquid-phase mass-transfer coefficient (m/s)
k_La = volumetric liquid-phase mass-transfer coefficient (s^{-1})
m = ratio of solubility in the liquid phase and in the gas phase
m_R = ratio of the gas solubility in the dispersed phase to that in the continuous phase
n = number of moles
N = impeller speed (s^{-1})
p = partial pressure (bar)
P = power input (W)
P_g = gassed power input (W)
R = gas constant [8.314 J/(mol K)]
R_X = reaction rate [mol/(m^3 s)]
S = spreading coefficient (N/m)
T = temperature (K)
T_V = vessel diameter (m)
u_G = superficial velocity (m/s)
V = volume (m^3)
W = impeller blade width (m)

Y, Y_{D1} = quantities used in eqs 20 and 25

Greek Letters

ϵ = phase fraction
μ = viscosity [kg/(m s)]
π = interfacial pressure (N/m)
ρ = density (kg/m^3)
σ = surface/interfacial tension (N/m)
τ_p = penetration time (s)
Φ = flow rate (m^3/s)

Subscripts

0 = initial value
C = with respect to the continuous phase
D = with respect to the dispersed phase
eq = at equiblibrium
G = with respect to the gas phase
i = at the interface
L = with respect to the liquid phase
W = of water

Literature Cited

(1) Kuntz, E. G. (Rhône Poulenc). French Patents FR 2.349.562, FR 2.366.273, and FR 2.733.516, 1976.

(2) Kroschwitz, J. I.; Howe-Grant, M. *Kirk Othmer, Encyclopedia of Chemical Technology*; Wiley: New York, 1996, Vol. A17.

(3) Kohlpaintner, C. W.; Fisher, R. W.; Cornils, B. Aqueous biphasic catalysis: Ruhrchemie/Rhône Poulenc oxo process. *Appl. Catal. A: Gen.* **2001**, *221*, 219.

(4) Cornils, B.; Kuntz, E. G. Introducing TPPTS and related ligands for industrial biphasic processes. *J. Organomet. Chem.* **1995**, *502*, 177.

(5) Wachsen, O.; Himmler, K.; Cornils, B. Aqueous biphasic catalysis: Where the reaction takes place. *Catal. Today* **1998**, *42*, 373.

(6) Cornils, B.; Hermann, W. A.; Eckl, R. W. Review: industrial aspects of aqueous catalysis. *J. Mol. Catal. A: Chem.* **1997**, *116*, 27.

(7) Yang, C.; Mao, Z.-S.; Wang, Y.; Chen, J. Kinetics of hydroformylation of propylene using RhCl(CO)(TPPTS)$_2$/TPPTS complex catalyst in aqueous system. *Catal. Today* **2002**, *74*, 111.

(8) Cents, A. H. G. Mass transfer and hydrodynamics in stirred gas−liquid−liquid contactors. Ph.D. Thesis, University of Twente, Enschede, The Netherlands, 2003.

(9) Calderbank, P. H. Physical rate processes in industrial fermentation. part I: The interfacial area in gas−liquid contacting with mechanical agitation. *Trans. Inst. Chem. Eng.* **1958**, *36*, 443.

(10) Hughmark, G. A. Power requirements and interfacial area in gas−liquid turbine agitated systems. *Ind. Eng. Chem. Process Des. Dev.* **1980**, *19*, 638.

(11) Greaves, M.; Barigou, M. Estimation of gas hold-up and impeller power in a stirred vessel reactor. In *Fluid Mixing III: A Three-Day Symposium (European Federation of Chemical Engineers)*; Harnby, N., Ed.; Institution of Chemical Engineers Symposium Series No. 108; Taylor & Francis: London, 1988; pp 235−255.

(12) Linek, V.; Mayrhoferová, J.; Mošnerová, J. The influence of diffusivity on liquid-phase mass transfer in solutions of electrolytes. *Chem. Eng. Sci.* **1970**, *25*, 1033.

(13) Llorens, J.; Mans, C.; Costa, J. Discrimination of the effects of surfactants in gas absorption. *Chem. Eng. Sci.* **1988**, *43*, 443.

(14) Cents, A. H. G.; Brilman, D. W. F.; Versteeg, G. F. Gas absorption in an agitated gas−liquid−liquid system. *Chem. Eng. Sci.* **2001**, *56*, 1075.

(15) Bhattacharya, A.; Chaudhari, R. V. An analysis of mass transfer effects in hydroformylation reactions. *Ind. Eng. Chem. Res.* **1987**, *26*, 1168.

(16) Bruining, W. J.; Joosten, G. E. H.; Beenackers, A. A. C. M.; Hofman, H. Enhancement of gas−liquid mass transfer by a dispersed second liquid phase. *Chem. Eng. Sci.* **1986**, *41*, 1873.

(17) Gerhartz, W.; Yamamoto, Y. S.; Campbella, F. T.; Pfefferkorn, R.; Rounsaville, J. F. *Ullmann's Encyclopedia of Industrial Chemistry*; Wiley-VCH: Weinheim, Germany, 1985; Vol. A4.

(18) Craig, V. S. J.; Ninham, B. W.; Pashley, R. M. The effect of electrolytes on bubble coalescence in water. *J. Phys. Chem.* **1993**, *97*, 10192.

(19) Cents, A. H. G.; Brilman, D. W. F.; Wijnstra, P. J.; Regtien, P. P. L.; Versteeg, G. F. Measuring bubble, drop and particle sizes in multiphase systems with ultrasound. *AIChE J.*, **2004**, *50*, 2750.

(20) Bartell, F. E.; Case, L. O.; Brown, H. The surface tension of mercury and of water in contact with saturated vapors. *J. Am. Chem. Soc.* **1933**, *55*, 2769.

(21) Lekhal, A.; Chaudhari, R. V.; Wilhelm, A. M.; Delmas, H. Gas−liquid mass transfer in gas−liquid−liquid dispersions. *Chem. Eng. Sci.* **1997**, *52*, 4069.

(22) Lorimer, J. W., Ed. *IUPAC Solubility Data Series*; Pergamon Press: Oxford, U.K., 1979; Vols. 5/6 and 43.

(23) Díaz, M.; Vega, A.; Coca, J. Correlation for the estimation of gas−liquid diffusivity. *Chem Eng. Commun.* **1987**, *52*, 271.

Received for review February 11, 2004
Revised manuscript received June 23, 2004
Accepted August 24, 2004

IE049888G